Ultrahigh-*Q* toroidal microresonators for cavity quantum electrodynamics

S. M. Spillane, T. J. Kippenberg, and K. J. Vahala
Thomas J. Watson Laboratory of Applied Physics, California Institute of Technology, Pasadena, California 91125, USA

K. W. Goh, E. Wilcut, and H. J. Kimble
Norman Bridge Laboratory of Physics, California Institute of Technology, Pasadena, California 91125, USA
(Received 27 August 2004; published 26 January 2005)

We investigate the suitability of toroidal microcavities for strong-coupling cavity quantum electrodynamics (QED). Numerical modeling of the optical modes demonstrate a significant reduction of the modal volume with respect to the whispering gallery modes of dielectric spheres, while retaining the high-quality factors representative of spherical cavities. The extra degree of freedom of toroid microcavities can be used to achieve improved cavity QED characteristics. Numerical results for atom-cavity coupling strength g, critical atom number N_0, and critical photon number n_0 for cesium are calculated and shown to exceed values currently possible using Fabry-Perot cavities. Modeling predicts coupling rates $g/2\pi$ exceeding 700 MHz and critical atom numbers approaching 10^{-7} in optimized structures. Furthermore, preliminary experimental measurements of toroidal cavities at a wavelength of 852 nm indicate that quality factors in excess of 10^8 can be obtained in a 50-μm principal diameter cavity, which would result in strong-coupling values of $(g/(2\pi), n_0, N_0) = (86\ \mathrm{MHz}, 4.6\times10^{-4}, 1.0\times10^{-3})$.

DOI: 10.1103/PhysRevA.71.013817 PACS number(s): 42.50.Pq, 32.80.−t, 42.50.Ct, 42.60.Da

I. INTRODUCTION

The use of an optical microcavity can greatly enhance the interaction of an atom with the electromagnetic field such that even a single atom or photon can significantly change the dynamical evolution of the atom-cavity system [1]. Achieving the regime of "strong coupling" [2,3] is critically dependent on the characteristics of the optical cavity and generally requires the optical modes to be confined in a small mode volume for extended periods of time (or equivalently high Q factor).

Recent experimental realizations of strong coupling have employed high-finesse Fabry-Perot (FP) optical microcavities [4–9]. Our experiments at Caltech include the realization of an "atom-cavity microscope" with a single atom bound in orbit by single photons [4] and the development of a laser that operates with "one and the same" atom [10]. Fabry-Perot cavities, while possessing ultrahigh-quality factors and finesse, are difficult to manufacture and control, requiring sophisticated dielectric mirror coatings as well as accurate feedback for resonant wavelength control. Due in part to these reasons, there has been increased interest in other microcavity systems which not only can address some or all of the limitations of Fabry-Perot cavities, but which in principle can have improved optical properties.

Based upon the pioneering work of Braginsky and colleagues [11], whispering-gallery-mode cavities have also been investigated for cavity QED (CQED) experiments for many years [12]. Experimental studies have demonstrated Q factors approaching 10^{10} in a silica microsphere whispering gallery cavity [13,14], with values exceeding 10^8 readily achievable over a broad range of cavity diameters and wavelengths. The combination of their very low cavity losses, small mode volumes, and their relative ease of fabrication makes them promising candidates for experiments in CQED [15,16]. Furthermore, the ability to couple these cavities with record coupling efficiencies to an optical fiber [17] (the medium of choice for low-loss transport of classical and nonclassical states [18]) is fundamentally important in CQED and bears promise for realizing quantum networks.

Recently, a new type of whispering-gallery-mode optical microcavity was demonstrated, which not only retains the high-quality factors of spherical cavities, but also has significant advantages in fabrication reproducibility, control, and mode structure. These cavities consist of a toroidally shaped silica cavity supported by a silicon pillar on a microelectronic chip [19]. The toroidal cavity shape allows an extra level of geometric control over that provided by a spherical cavity and thus begs the question as to how these structures compare with silica microspheres and other microcavity designs for strong-coupling cavity QED. In this paper we numerically investigate the suitability of toroidal microcavities for strong-coupling cavity QED experiments, and for purposes of comparison, we focus on the interaction with atomic cesium [4,20]. We show that toroid microcavities can achieve ultrahigh-quality factors exceeding 10^8 while simultaneously obtaining very large coupling rates between the cavity and a cesium atom. It is found that these cavities not only surpass the projected limits of FP technology [20], but also either exceed or compare favorably to other cavity designs such as photonic band-gap devices [21,22]. Last, we present preliminary experimental measurements of quality factors for toroidal cavities at a wavelength of 852 nm, suitable for strong-coupling CQED with atomic cesium. These results show that currently attainable Q values are already quite promising.

II. STRONG COUPLING IN AN ATOM-CAVITY SYSTEM

The coupling rate g between an atomic system and an electromagnetic field is related to the single-photon Rabi fre-

quency $\Omega = 2g$ and can be expressed in terms of the atomic and cavity parameters by [1]

$$g(\mathbf{r}) = \gamma_{\perp} |\vec{E}(\mathbf{r})/\vec{E}_{\max}| \sqrt{V_a/V_m}, \tag{1}$$

$$V_a = 3c\lambda^2/(4\pi\gamma_{\perp}), \tag{2}$$

where $\gamma_{\perp}$ is the transverse atomic dipole transition rate, $|\vec{E}(\mathbf{r})/\vec{E}_{max}|$ denotes the normalized electric field strength at the atom's location $\mathbf{r}$, V_a is a characteristic atomic interaction volume (which depends on the atomic dipole transition rate, the transition wavelength λ, and the speed of light c), and V_m is the cavity-electromagnetic-mode volume. Assuming the atom interacts with the electromagnetic field for a time T, strong atom-field coupling occurs if the rate of coupling exceeds all dissipative mechanisms—i.e., $g \gg (\kappa, \gamma_{\perp}, T^{-1})$. In this expression κ denotes the cavity field decay rate, given in terms of the cavity quality factor Q by $\kappa \equiv \pi c/(\lambda Q)$. The degree of strong coupling can also be related to a set of normalized parameters [1],

$$n_0 \equiv \gamma_{\perp}^2/(2g^2), \tag{3}$$

$$N_0 \equiv 2\gamma_{\perp}\kappa/(g^2), \tag{4}$$

where n_0 is the critical photon number, which is the number of photons required to saturate an intracavity atom, and N_0 is the critical atom number, which gives the number of atoms required to have an appreciable effect on the cavity transmission. Note that $(N_0, n_0) \ll 1$ provides a necessary but not sufficient condition for strong coupling.

Examining these parameters, we see that only the critical atom number $N_0 \propto V_m/Q$ is dependent on the cavity-loss rate (or equivalently Q factor). It is the possibility of realizing extremely low critical atom numbers with ultrahigh-Q microcavities that has fostered the investigation of silica microspheres for strong-coupling CQED experiments. However, the geometry of a spherical dielectric dictates a definite relationship between cavity-mode volume V_m and the associated quality factor Q and, hence, of the value of the coupling parameter $g \propto V_m^{-1/2}$ while still maintaining ultrahigh-quality factors [23]. This is a result of the fact that to achieve large atom-cavity coupling rates (comparable to or exceeding those of FP cavities) the cavity diameter must be made small [8-μm-diameter sphere gives $g/(2\pi) \approx 740$ MHz] in order to both lower the modal volume and to increase the electric field strength at the atomic position (assumed to be the cavity surface at the point of maximum electric field strength). However, at the optimum radius for atom-coupling strength, the tunneling loss of the microcavity results in a low achievable Q factor ($Q \approx 4 \times 10^4$), thereby raising the critical atom number. While the relatively large mode volumes of silica microsphere cavities preclude them from competing with ultrasmall mode volume cavities (such as photonic band-gap cavities) on the basis of coupling strength alone, there is the possibility to access simultaneously both ultrahigh-Q and small mode volume, using toroidal microresonators.

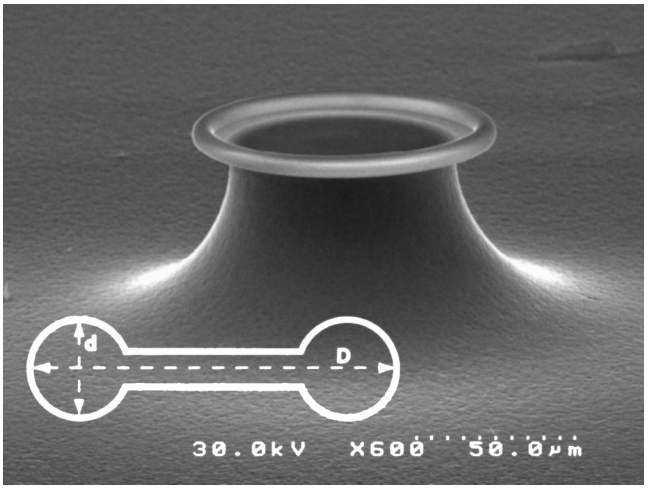

FIG. 1. Scanning electron micrograph of a toroidal microcavity. The principal and minor diameters are denoted by D and d, respectively.

III. TOROIDAL MICRORESONATORS

Toroidal microresonators are chip-based microcavities that possess ultrahigh-Q ($>10^8$) whispering-gallery type modes [19]. The realization of ultrahigh-Q chip-based resonators allows improvements in fabrication and control, while additionally allowing integration with complementary optical, mechanical, or electrical components. In brief, these resonators are fabricated by standard lithographic and etching techniques, followed by a laser-reflow process, as outlined in Ref. [19]. The combination of thermal isolation of the initial preform periphery and thermal heat sinking of the preform interior through the strong heat conduction of the silicon support pillar results in a preferential melting of the preform along the disk periphery under CO_2 laser irradiation. Surface tension then induces a collapse of the silica disk preform, resulting in a toroidally shaped boundary, with the final geometry controlled by a combination of irradiation flux and exposure time. Importantly, as the optical mode resides in the extremely uniform and smooth (reflowed) periphery of the structure, the quality factors of optical whispering-gallery modes can achieve ultrahigh-Q performance, exceeding 10^8. Figure 1 shows a scanning electron micrograph of the side view of a typical toroidal microcavity. Quality factors as high as 4×10^8 at a wavelength of 1550 nm (corresponding to a photon lifetime of $\sim$300 ns) have been measured [24].

IV. MICROTOROID NUMERICAL MODELING

In order to investigate the properties of microtoroids for CQED, this paper will focus on the D_2 transition of cesium which occurs at a wavelength of 852.359 nm ($\gamma_{\perp}/2\pi \approx 2.6$ MHz) [20], with scaling to other systems accomplished in the fashion of Ref. [23]. Fundamentally, the coupling between an atom and a cavity field can be specified by four parameters: the atomic transition moment, the cavity field strength at the atom's location, the cavity mode volume V_m, and the cavity quality factor Q. Since the optical modes

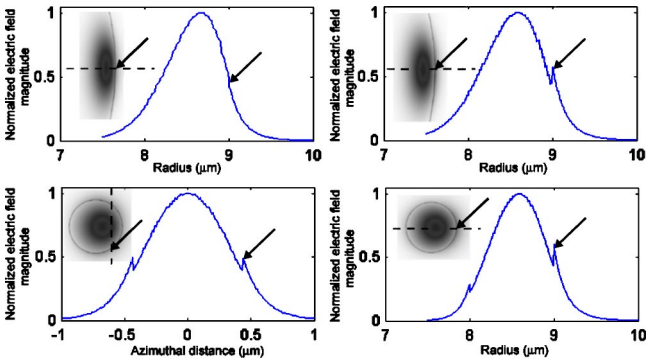

FIG. 2. Electric field magnitude for the whispering-gallery modes of a spherical (top row) cavity of diameter 18 μm and a toroidal cavity (bottom row) with principal diameter of 18 μm and a minor diameter of 1 μm. The left (right) column shows the TE- (TM-) polarized mode near 850 nm. The arrows indicate the location of the maximum external electric field strength, where we assume the atom is located. The dotted lines in the two-dimensional field distribution indicate the cross section where the electric field is displayed.

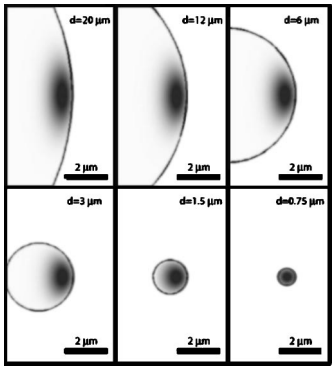

FIG. 3. Electric field profiles for a toroidal cavity with a principal diameter $D=20$ μm and minor diameters $d=20$, 12, 6, 3, 1.5, and 0.75 μm. The calculations correspond to a TM-polarized mode near 850 nm. The optical mode behaves as a whispering-gallery-type mode until the minor diameter is below approximately 1.5 μm, at which point the mode approaches that of a step-index optical fiber [28].

are confined to the interior dielectric in whispering-gallery-type resonators, the atom can interact only with the evanescent field of the cavity mode. In the following discussion, the atom is assumed to be located near the resonator surface at the location where the electric field strength is largest, as illustrated in Fig. 2. For TM-polarized modes (defined such that the dominant electric field component is in the radial direction) this occurs at the outer cavity boundary in the equatorial plane, while for TE-polarized modes (dominant electric field component in the azimuthal-vertical direction) the location of the maximum external field strength is more complicated. As the toroidal geometry is compressed with respect to a sphere (i.e., reducing the ratio of minor-to-principal toroid diameter), the maximum field strength for a TE-polarized mode changes from the equatorial outer cavity boundary to approaching the azimuthal axis (see Fig. 2). While the precise localization of the atom at the cavity evanescent field maximum has been analyzed in detail [25,26], such localization has not yet been achieved experimentally. Nonetheless, this assumption allows a simple way to characterize the relative merit of this cavity geometry with respect to other cavity designs. Also, in what follows we will only consider the fundamental radial and azimuthal modes for both polarizations (TE and TM), as they possess the smallest modal volumes and thus the highest coupling strengths.

The microtoroid geometry, which exhibits a dumbbell-shaped cross section, can in most cases be considered a torus, as the presence of the supporting disk structure only affects the optical mode when the torus diameter becomes comparable to the radial extent of the optical mode. As shown in Fig. 3, this point occurs when the toroid minor diameter (i.e., the cross-sectional diameter of the torus) is below approximately 1.5 μm for a principal diameter of 16 μm. Furthermore, through improvements in fabrication the influence of the toroid support can in principle be minimized. In contrast to FP and microsphere cavities, the optical modes of a toroid do not possess analytic solutions. While one can derive approximate expressions for the optical behavior of these structures for both the low transverse compression (spherelike) and high transverse compression (step-index, fiberlike) regimes, we are mostly interested in the intermediate geometrical regimes, as these are both experimentally accessible and retain the most desirable properties of whispering-gallery-type microcavities. To accomplish this task, a two-dimensional finite-element eigenmode-eigenvalue solver was used to characterize the optical modes of the cavity over the complete geometrical range, after explicitly accounting for the rotational symmetry. The optical modes were calculated in a full-vectorial model, which provides the complete electric field dependence. The accuracy of the numerical technique was carefully verified by comparison with results using the analytical solution for a microsphere cavity [27]. The results for the mode volumes, resonance wavelengths, and field profiles were in good agreement (fractional error was less than 10^{-4} and 10^{-2} for the resonance wavelength and modal volume, respectively). Furthermore, the error in the radiation quality factor was less than 10% over a wide value of radiation Q's (10^3–10^{14}), demonstrating that this method can give the accuracy required to investigate the fundamental radiation-loss limits in the cavity geometries of interest in this work. Due to the fact that for smaller cavity geometries the resonance wavelengths do not necessarily coincide with the cesium transition of interest, the data in this work were evaluated by using values calculated at the closest resonance wavelengths, both blueshifted and redshifted with respect to the desired resonance, to extrapolate values at the desired wavelength (the mode volumes were linearly extrapolated and the radiation quality factors exponentially extrapolated as a function of wavelength).

A. Mode volume

The optical-mode volume is determined by

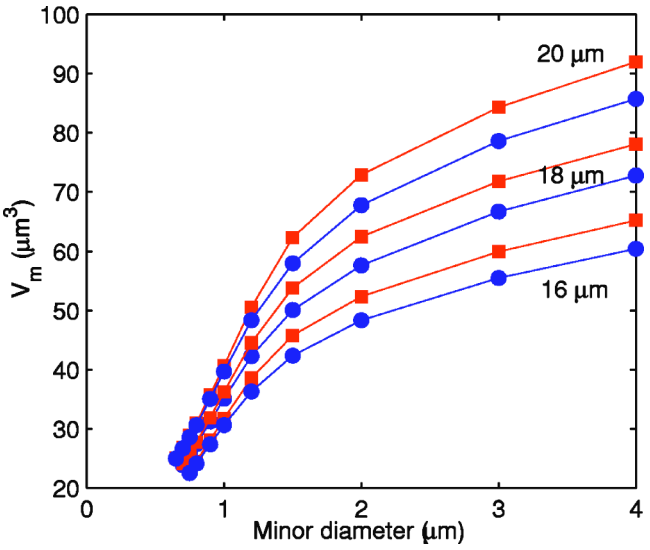

FIG. 4. Calculated mode volumes for a silica toroidal microresonator versus minor diameter for principal diameters of 20, 18, and 16 μm. The plot shows both TM (squares) and TE (circles) polarizations. As the minor diameter is reduced a slow reduction of modal volume due to confinement in the azimuthal direction occurs, followed by a fast reduction for large confinement when the optical mode is strongly compressed in both the radial and azimuthal directions.

$$V_m \equiv \frac{\int_{V_Q} \epsilon(\vec{r})|\vec{E}(\vec{r})|^2 d^3\vec{r}}{|\vec{E}_{\max}|^2}, \tag{5}$$

where V_Q represents a quantization volume of the electromagnetic field and $|\vec{E}|$ is the electric field strength [26]. In these calculations, we have chosen the quantization volume cross section to consist of a square region of approximately 10 μm width and height centered about the radial cavity boundary. This choice allows the mode volume to be determined to a good accuracy while minimizing computational requirements. As a further confirmation of the validity of this approach, we note that the radiation loss is weak for the range of geometries modeled in this work, resulting in only a marginal difference in the numerically calculated mode volume for different choices of quantization volume.

Figure 4 shows the calculated modal volume for the fundamental mode of a toroidal cavity as a function of minor diameter and for principal diameters ranging from 16 to 20 μm. For clarity, only data for minor diameters below 4 μm are shown. Both TM (squares) and TE (circles) polarizations are shown. The calculations show a reduction of modal volume for both polarizations as the toroid minor diameter is decreased. This is expected when considering the additional confinement provided by the toroid geometry beyond the spherical geometry, as illustrated in the electric field plots of Fig. 3. As the minor diameter is decreased, there is initially a slow reduction of modal volume, which agrees very well with a simple model that accounts for transverse guiding (azimuthal direction) using an approximate one-dimensional harmonic oscillator model. This approach results in a reduction of modal volume which scales as $(d/D)^{1/4}$ with respect to that of a spherical cavity. This formula holds for minor diameters greater than approximately 2 μm for the principal diameters considered in this work. For smaller diameters, the spatial confinement becomes strong enough that the optical mode is additionally compressed in the radial direction. This results in a faster reduction of modal volume, with the optical modes approaching those of a step-index optical fiber (this occurs for a minor diameter below approximately 1 μm) [28]. The mode volume reduces until the point where the optical mode becomes delocalized due to the weak geometrical confinement, causing a finite minimum value. Determination of the exact point of the minimum modal volume upon reduction of minor diameter (for a fixed principal diameter) can be uncertain, as the choice of quantization volume now plays a critical role (as discussed above). For this reason the results in Fig. 4 show the modal volume only for inner diameters down to 0.65 μm, where mode volume determination was unambiguous.

Calculation of the modal volume and the maximum electric field amplitude at the exterior cavity equatorial boundary is straightforward, giving a simple way to calculate both the coupling strength and the critical photon number. In order to obtain the cavity decay rate κ and the critical atom number N_0, however, the cavity Q factor must be determined.

B. Quality factor

The radiation loss of the optical modes of a spherical cavity is easily found by consideration of the analytic characteristic equation [29]

$$n^{1-2b}\frac{[nkRj_\ell(nkR)]'}{nkRj_\ell(nkR)} = \frac{[kRh_\ell^{(1)}(kR)]'}{kRh_\ell^{(1)}(kR)}, \tag{6}$$

where n is the refractive index of the spherical cavity (the external index is assumed to be unity), R is the cavity radius, b represents the polarization of the optical mode (1 for TM and 0 for TE), and j_ℓ ($h_\ell^{(1)}$) represents the spherical Bessel (Hankel) function. The prime denotes differentiation with respect to the argument of the Bessel (Hankel) function. This equation accounts for radiation loss through the use of an outgoing wave outside the cavity, as given by the complex Hankel function of the first kind. Solution of this equation results in a complex wave number $k=k_{Re}+ik_{Im}$, which determines both the resonance wavelength ($\lambda=2\pi/k_{Re}$) and the radiation quality factor [$Q_{rad}=k_{Re}/(2k_{Im})$].

However, while the spherical solution can provide some insight into the scaling of the radiation quality factor for toroidal cavities where the minor diameter is large (sphere like), the radiation loss when the optical mode is strongly confined (as represented by small minor diameters) is expected to decrease much more rapidly. Figure 5 shows numerical calculations of the radiative quality factor as the minor diameter is decreased for various principal diameters of 16, 18, and 20 μm. We observe an initially slow reduction of the radiative quality factor in the geometrical regime where the minor diameter exceeds the radial extent of the optical

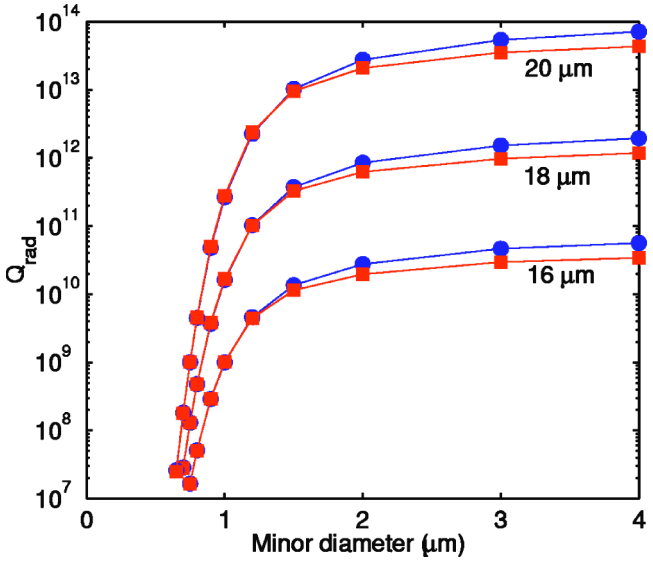

FIG. 5. Calculated radiation loss for a toroidal microcavity as a function of minor diameter, for principal diameters of 20, 18, and 16 μm. Both TM (squares) and TE (circles) polarizations are shown. The data show a slow reduction of Q as the minor diameter is reduced while the mode behaves primarily as a whispering-gallery-type mode. However, as the geometrical confinement increases to such a point as the optical mode approaches that of a step-index fiber, there is a significant reduction of the quality factor.

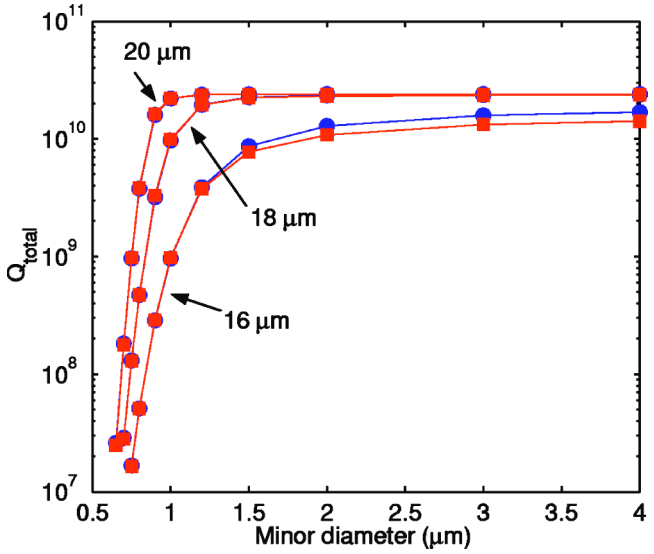

FIG. 6. Total quality factor for a toroidal microcavity versus minor diameter for principal diameters of 16, 18, and 20 μm. Both TE (circles) and TM (squares) polarizations are shown. The total quality factor is composed of the radiative quality factor from Fig. 5 along with the silica-absorption-limited $Q_{mat}=2.4\times10^{10}$ at a wavelength of 852 nm. The plots indicate that the total quality factor is limited by silica absorption when the principal diameter is larger than 16 μm and the minor diameter is larger than approximately 1 μm. Furthermore, both polarizations have similar quality factors over the range of geometries studied.

mode (i.e., where the optical mode exhibits whispering-gallery behavior). As the minor diameter is reduced to a level comparable to or smaller than the radial extent of the optical mode (step-index fiber like regime), the drop-off of the radiative Q is much more dramatic, with a decrease of over an order of magnitude for a reduction of inner diameter of just 50 nm.

The total optical loss of a cavity has contributions not only from radiation loss, but also includes other dissipative mechanisms, such as intrinsic material absorption, losses resulting from both surface and bulk scattering, and losses stemming from contaminates on the resonator surface [30]. One of the dominant contaminates which adversely affects the cavity Q is OH and water adsorbed onto the cavity surface. While prior investigations of these loss mechanisms have resulted in approximate expressions for water absorption and surface scattering [14,31], only very large resonators were studied, as opposed to the much smaller diameter cavities studied in this work. To obtain an improved estimate of the effect of water on the small diameter cavities in this paper, a simple model was used which determines the fraction of optical energy absorbed by a monolayer of water located at the cavity surface. This method gives an estimated quality factor for a monolayer of water to be greater than 10^{10} for the case of a spherical resonator with a principal diameter of 50 μm. While the water-limited quality factor will be slightly lower for the smaller principal diameter cavities in this work and also slightly lower due to the increased overlap between the optical mode and the cavity surface in a toroidal geometry, these values are comparable to the quality factor due solely to the intrinsic absorption of silica in the 800-nm wavelength band. As in principle with proper fabrication the presence of water and OH can be prevented, with surface scattering minimized, we will focus only on the contributions from intrinsic silica absorption and radiation loss. These two mechanisms put a fundamental limit on the Q possible in these structures.

Figure 6 shows the calculated total quality factor for various principal toroid diameters in the range of 16–20 μm, as a function of the minor diameter. The total quality factor is calculated through the relation $1/Q_{total}=1/Q_{rad}+1/Q_{mat}$, where only radiation loss and silica absorption are included. For principal diameters less than 18 μm, there is a monotonic decrease in quality factor as the minor diameter is decreased. This is a result of the whispering-gallery-loss increase due to the additional confinement. For larger principal diameters, the overall quality factor is clamped near the limiting value resulting from silica absorption for most minor diameters (with only a slight decrease as minor diameter is reduced), until the minor diameter is small enough that the radiative quality factor decreases below the quality factor due to silica absorption. For the principal diameters studied in this work, this point occurs as a minor diameter of around 1 μm.

C. Cavity QED parameters

The determination of the coupling strength from the modal volume follows from Eq. (1). Figure 7 shows the

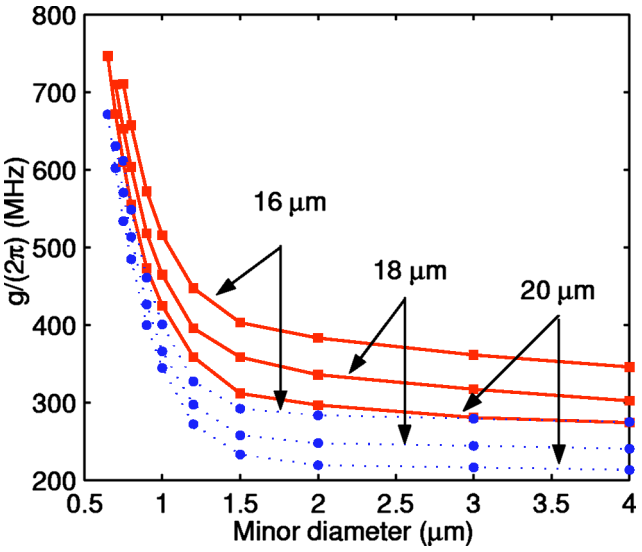

FIG. 7. Atom-cavity coupling parameter g vs minor diameter for toroidal cavities having a principal diameter of 16, 18, and 20 μm, with g increasing for smaller principal diameters. Both TE (circles) and TM (squares) polarizations are shown. The plots indicate that the coupling strength increases dramatically as the minor diameter decreases below 1.5 μm, which is a result of the rapid reduction of mode volume and the increased electric field strength at the cavity surface.

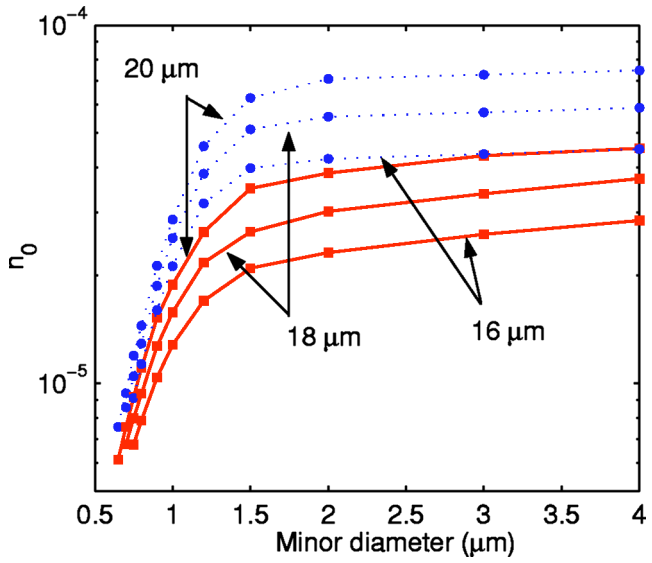

FIG. 8. Critical photon number n_0 vs minor toroid diameter for a cavity with principal diameters of 16, 18, and 20 μm. Both TE (circles) and TM (squares) polarizations are shown. The plots show that as both toroid principal diameter and minor diameter are reduced, the critical photon number decreases. This follows directly from the behavior of the atom-cavity coupling parameter g, as indicated in Fig. 7. The calculations show that critical photon numbers of 6×10^{-6} are possible (with quality factors exceeding 10^7).

atom-cavity coupling rate $g/(2\pi)$ for various toroid principal diameters as the toroid minor diameter is decreased. It can be seen that there is a monotonic rise in g for higher-aspect-ratio toroids (i.e., D/d), as a direct result of the compression of modal volume. The rate of increase of g as the minor diameter is reduced increases dramatically as the toroid geometry transitions from a whispering-gallery-type mode to a strongly confined step-index fiber-type mode. This is due not only to the faster rate of reduction of mode volume in the step-index fiber like regime as the minor diameter is decreased, but also due to the increase in electric field strength at the cavity surface [as $g\propto|E|(V_m)^{-1/2}$]. Note that the coupling strengths shown do not correspond to the absolute maximum for these structures, as this work has focused on the simultaneous realization of high-quality factors and small modal volume. Therefore, mode volumes were calculated only down to where the radiation quality factor is equal to or slightly exceeds 10^7. Also, as mentioned previously, by making this restriction we prevent any uncertainty in the calculated mode volumes (and hence g) through the definition of the modal quantization volume. Under these assumptions, the calculations indicate that coupling parameters exceeding 700 MHz are possible.

Figure 8 shows the corresponding critical photon numbers (n_0). The results reveal that values as low as 6×10^{-6} are possible, with the associated quality factors exceeding 10^7. As will be discussed in more detail in the next section, this value is not only comparable to the fundamental limit of FP technology, but also vastly exceeds that possible for fused silica microspheres with a comparable quality factor.

One of the primary reasons high-Q whispering-gallery-mode cavities are promising for CQED is their very low critical atom number. Figure 9 shows the calculated critical atom number versus minor diameter for toroid principal diameters of 16, 18, and 20 μm. The plot shows that for the larger principal diameters of 18 and 20 μm there is a minimum in the critical atom number as the toroidal minor diam-

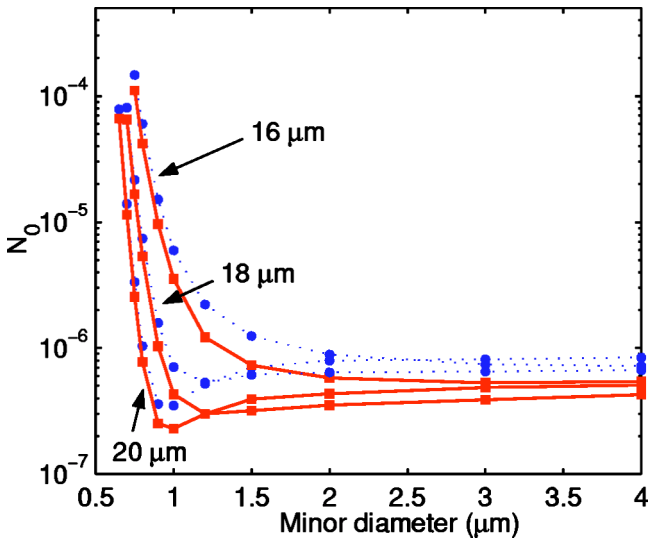

FIG. 9. Critical atom number N_0 vs minor diameter for a toroidal microcavity with principal diameters of 16, 18, and 20 μm. For small minor diameters the critical atom number decreases as the principal diameter increases. Both TE (circles) and TM (squares) polarizations are shown. The plots indicate that there is a minimum value of the critical atom number near 2×10^{-7} for a toroidal cavity with a principal diameter of 20 μm and an inner diameter of 1 μm (TM mode).

eter is reduced. The minimum occurs near a minor diameter of 1 μm. This minimum arises from the clamping of the total quality factor (to the quality factor resulting from silica absorption) for larger minor diameters when the principal diameter is greater than approximately 18 μm. Thus, by reducing the minor diameter for a fixed principal diameter, the quality factor is nearly unchanged while the coupling strength is monotonically increasing. The critical atom number decreases until the region where the minor diameter is such that the overall Q is determined by whispering-gallery loss. At this point the critical atom number increases approximately exponentially. The plot for the 20 μm principal diameter shows that in a toroidal geometry slightly larger principal diameters can offer some benefit, as the minor diameter can be compressed more strongly while maintaining high radiative quality factors and, thereby, lowering the critical atom number. A critical atom number of approximately 2×10^{-7} is possible using a toroid principal diameter of 20 μm and a minor diameter of 1 μm.

V. EXPERIMENTAL MEASUREMENT OF MICROTOROIDS FOR STRONG-COUPLING CAVITY QED AT 852 nm

The presented numerical results indicate that toroidal cavities can theoretically obtain high values of atom-cavity coupling while simultaneously retaining an extremely low critical photon number and in particular an exceedingly small critical atom number. While in principle the critical atom number can be more than 100 times smaller than any currently demonstrated cavity, the necessity of realizing material-limited quality factors exceeding 2×10^{10} is experimentally challenging. The current record for any cavity is 9×10^{9} [14], in a large-diameter microsphere cavity, whereas for toroidal cavities quality factors as high as 4×10^{8} at a resonance wavelength of 1550 nm have been realized [24]. However, for cavity quality factors much larger than 10^{8}, the dominant dissipative mechanism in the atom-cavity system is the radiative decay rate of the atomic medium, which is 2.61 MHz for the D_2 transition of cesium. For this reason more "modest" quality factors, in the range of current experimentally achievable values (e.g., a few hundred million) are attractive. As these values are currently realizable for toroidal cavities at a wavelength of 1550 nm, we have investigated experimentally the quality factors and fabrication limits for structures designed for strong coupling to the cesium transition at a wavelength of 852 nm.

As toroidal cavities are fabricated using a combination of lithography and a silica reflow process, the advantages of lithographic control and parallelism are obtained and, in fact, are a significant step forward over spherical cavities. As the shape of the initial silica preform dictates the maximum possible principal and minor diameter and is lithographically formed, precise control of the geometry dimensions is possible. Reproducible principal diameters ranging from >100 to 12μm have been fabricated. This lower value, while currently dictated by the available laser power in our setup, is sufficient to obtain the range of principal diameters optimally suited for CQED, as indicated above. While the capability to obtain reproducible principal diameters is a significant improvement over spherical cavities, the ability to accurately control the minor diameter is particularly important to CQED. As noted previously [19], the final minor diameter of the fabricated structures is a result of a combination of factors, which are the initial silica preform thickness, the supporting pillar size, and the laser irradiation intensity and duration. Minor diameters as small as 3 μm at principal diameters as low as 12 μm have been realized experimentally.

We have measured the quality factor of a series of fiber-taper-coupled toroidal microcavities at a wavelength of 852 nm, using an experimental apparatus similar to previous work [19,32]. The excitation laser was a New Focus Vortex laser with a tunability of 40 GHz with a center wavelength of 852.359 nm. The laser output was double passed through an acousto-optic modulator for the purpose of performing a cavity ringdown measurement. The resulting beam was able to be extinguished by a TTL electrical control signal, with a corresponding optical decay time of 15 ns. This beam was then coupled into a single-mode 850 nm fiber and subsequently interacted with the toroidal resonators through the tapered portion of the fiber. Due to the limited tuning range of the excitation laser (which is less than the free-spectral range between fundamental modes in the cavity principal diameters of interest), overlap of a fundamental resonance with the laser wavelength range was difficult. Obtaining an optical fundamental mode at 852.359 nm was achieved by thermally shifting the optical resonance through the use of a Peltier heating element, which allowed tuning of the cavity resonance by up to approximately 50 GHz. Upon realization of a fundamental cavity resonance at the proper wavelength, the intrinsic quality factor was inferred two ways (Fig. 10): through cavity ringdown [19] and through the threshold for stimulated Raman scattering [32]. The results of both measurements were in agreement and resulted in a measured quality factor as high as $Q_{total}=1.2\times10^{8}$ in a cavity with a principal diameter of 50 μm and a minor diameter of 6 μm. For this cavity geometry, the whispering-gallery loss is negligible ($Q_{rad}\approx10^{36}$) compared to the intrinsic silica absorption loss, such that the overall theoretical quality factor can be as high as $Q_{total}\approx2\times10^{10}$. We expect upon further measurements that this quality factor can be increased to levels comparable to measurements performed at a wavelength of 1550 nm (4×10^{8}).

While this cavity geometry is far from the optimal geometry suggested in this paper, this structure was chosen in order to increase the likelihood of finding a fundamental resonance at 852 nm. Even for this relatively large structure, cavity QED parameters of $(g/(2\pi),n_0,N_0)=(86\ \mathrm{MHz},4.6\times10^{-4},1.0\times10^{-3})$ are calculated. Comparison of these values to current FP cavities [4,10,20] indicates that even without additional improvements in fabrication these results are close in coupling strength and improved with respect to the critical atom number. Additionally, if we restrict the geometry and overall quality factor to values which are currently realizable (i.e., a quality factor of 10^{8} at a wavelength of 852 nm with a minor diameter of 3.5 μm, which represents a reasonably comfortable margin from the actual current limits), the optimal principal diameter is 13 μm (this geometry

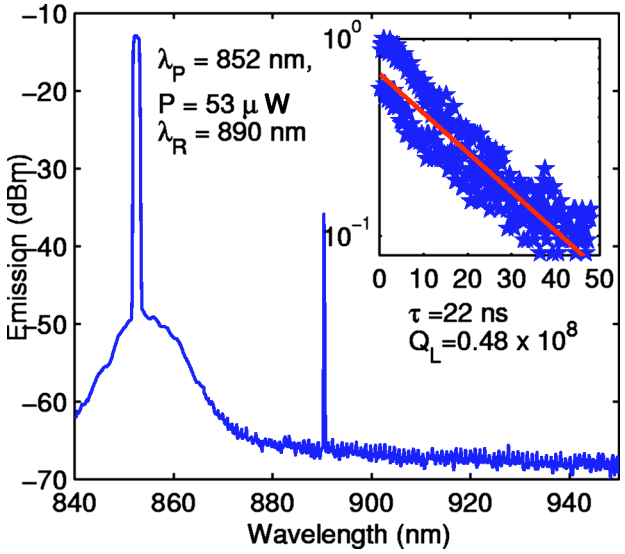

FIG. 10. Experimental measurement of the intrinsic quality factor for a toroidal microresonator at a resonance wavelength of 852 nm. The main figure shows the generation of stimulated Raman scattering, illustrated by the secondary peak located at a wavelength of 890 nm. The threshold pump power for stimulated Raman scattering (53 μW) can be used to infer the intrinsic quality factor of 1×10^8 for this cavity. The inset shows the temporal cavity decay resulting from a series of ringdown measurements for a different toroidal microcavity. The measured photon lifetime of $\tau=22$ ns corresponds to a loaded quality factor of $Q_L=0.48\times10^8$. After correcting for fiber-taper loading and the presence of backscattering, an intrinsic quality factor of 1.2×10^8 is obtained.

has a radiative quality factor of 1.8×10^8). For these values the TM-polarized optical mode would have CQED parameters of $(g/(2\pi),n_0,N_0)=(450\ \text{MHz},1.7\times10^{-5},4.5\times10^{-5})$, which are far superior to current FP cavities.

VI. COMPARISON OF MICROTOROIDS WITH OTHER RESONATORS FOR CAVITY QED

Table I presents a comparison of CQED parameters for various cavity types including toroidal, FP, and photonic crystal. To date, most experimental work has involved the use of Fabry-Perot cavities, with current state-of-the-art fabrication technology allowing the attainment of coupling strengths of 110 MHz, with corresponding critical atom numbers of 6×10^{-3} [4]. Estimates on the theoretical performance limits of FP cavities have also been investigated [20], predicting coupling rates as large as 770 MHz, with a corresponding critical atom number of 2×10^{-4}. While this level of performance may be theoretically possible, the current necessity of expensive and sophisticated high-reflection dielectric mirror coatings does not bode well for easy improvements with respect to current technology. This is one of the reasons silica microspheres are of such high interest. Calculation of the limits possible with silica microspheres [23] shows that not only is it possible to obtain high values of atom-cavity coupling solely by changing the cavity diameter, which is easily in the realm of current fabrication capability, but their ultra high-quality factors result in significant improvement in the critical atom number (with values approaching 3×10^{-6} possible provided that silica absorption-limited quality factors can be obtained). Even using quality factors in the range of a few hundred million, which is already experimentally demonstrated, critical atom numbers around 10^{-4} are possible, which is comparable to the FP limit. From the analysis of the previous section, we see that toroidal cavities can attain coupling strengths comparable to or exceeding the best values possible for either FP or microsphere cavities, while at the same time providing much lower critical atom numbers. As discussed previously, this arises from the extra level of geometrical control possible in a toroidally shaped cavity, which allows one to retain both the high-coupling strength representative of small-mode volume cavities while preserving high-quality factors. Clearly this fact, along with other advantages in control and reproducibility over spherical cavities, suggests that these structures are promising for CQED experiments.

Last, a comparison with photonic band-gap (PBG) cavities is also provided in the table. Due to the realization of optical mode volumes near the fundamental limit in a dielectric cavity [21], combined with recent results demonstrating reasonably high-quality factors ($\sim$45 000) [33], these cavities are strong candidates for chip-based strong-coupling CQED [22]. While these structures can potentially achieve atom-cavity coupling strengths $g\gtrsim17$ GHz [22], far greater than those possible in a silica dielectric cavity, their much lower quality factors result in greater critical atom numbers than possible in toroidal microcavities. For example, the work of Ref. [22] projects $N_0=6.4\times10^{-5}$. We also note that the correspondingly lower quality factors also result in modest ratios of coupling to dissipation $g/\max(\gamma_\perp,\kappa)$ (a figure of merit indicative of the number of Rabi oscillations which occur) of $\sim$4 [22], much lower than predicted for toroidal structures ($\sim$165). Furthermore, we can consider an additional figure of merit: namely, the "rate of optical information per atom" [1], given by $R\equiv g^2/\kappa$. The table indicates that toroidal cavities compare favorably with PBG cavities in this figure of merit as well.

VII. CONCLUSION

Our work has demonstrated that toroidal resonators are promising cavities for investigation of the coupling of an atomic system to the electromagnetic field in the regime of strong coupling. Not only are these structures arguably simpler to manufacture and control than other structures such as microspheres and FP cavities, but also allow integration on a silicon chip, paving the way for the addition of atom traps [34] and waveguides which can enhance the capability and possibly reduce the experimental complexity of CQED studies. Furthermore, we note that in addition to the enhanced

TABLE I. Summary of the relevant parameters for cavity QED for a variety of resonator systems. The table shows both the experimental state of the art [23] and the projected limits for a Fabry-Perot cavity [20], plus current experimental results with silica microspheres [16]. Furthermore, a theoretical comparison between silica microspheres [23], photonic band-gap cavities [22], and toroidal microresonators (this work) is also given. The results indicate that toroidal cavities can uniformly exceed the performance on these parameters for both FP cavities and silica microspheres. Comparison with PBG cavities indicates that toroids possess much lower atom-cavity coupling strengths (as a result of their much larger mode volumes), but still result in greatly improved critical atom numbers due to their very large quality factors.

Resonator system	Coupling coefficient $g/(2\pi)$ (MHz)	Critical photon number n_0	Critical atom number N_0	Coupling to dissipation ratio $g/\max(\gamma_\perp,\kappa)$	Rate of optical information $R\equiv g^2/\kappa$ (Mbits/sec)
Fabry-Perot experimental state of the art	110	2.8×10^{-4}	6.1×10^{-3}	7.8	5.4×10^{3}
Fabry-Perot projected limits	770	5.7×10^{-6}	1.9×10^{-4}	36	1.7×10^{5}
Microsphere experimental ($D=120$ μm)	24	5.5×10^{-3}	3.0×10^{-2}	7.2	1.1×10^{3}
Microsphere theory					
Maximum g ($D=7.25$ μm)	750	6.1×10^{-6}	7.3×10^{-1}	0.01	4.5×10^{1}
Minimum N_0 ($D=18$ μm)	280	4.3×10^{-5}	3.1×10^{-6}	107	1.1×10^{7}
Photonic band-gap cavity	17000	7.6×10^{-9}	6.4×10^{-5}	3.9	5.1×10^{5}
Toroidal microcavity theory					
Maximum g	>700	6.0×10^{-6}	2.0×10^{-4}	40	1.6×10^{5}
Minimum N_0	430	2.0×10^{-5}	2.0×10^{-7}	165	1.6×10^{8}

performance benefit of having a toroidal geometry, the capability to retain a relatively large resonator diameter over other structures results in a smaller free-spectral range (FSR). This allows not only easier tuning of the cavity resonance location to correspond precisely to the atomic transition wavelength, but also may allow integration of a supplemental far-off-resonance trap by exciting the cavity at a multiple of the free-spectral range. The realization of a cavity with a smaller FSR may allow a closer matching of a secondary resonance location to the pump wavelength which corresponds to state-insensitive trapping of atomic cesium [7], which can simplify the atom-cavity dynamics. The use of a silica dielectric whispering-gallery cavity also allows operation over a broad range of wavelengths, with very-high-quality factors possible for nearly all resonances. This is in strong contrast to the mirror reflectivity limits of coated FP cavities.

The ability to connect distant quantum nodes with high efficiency, preferably over optical fiber, is very desirable for quantum networks. Using FP cavities, optical fiber coupling is possible; however, the overall coupling efficiency is modest ($\sim$70%). Fiber-taper-coupled microtoroids allow coupling efficiencies in excess of 99% [17], above both FP and PBG cavities (97%) [35]. This capability to obtain near-complete input and output coupling efficiencies strongly suggests the use of fiber-coupled silica whispering-gallery cavities, such as microtoroids, as building blocks to enable high-performance quantum networks.

As a further note, the use of higher-index contrast dielectric material can allow additional improvements in the performance of these structures. The use of silica as the dielectric of choice in both the spherical geometry and in the toroidal microcavities studied in this work was convenient, as these structures not only possess record high-quality factors but are currently producible. However, as the radiative quality factor of a whispering-gallery-type cavity is strongly dependent on the refractive index difference between the structure and external environment, much smaller modal volumes are possible for a given quality factor with the use of a higher-index resonator material. In fact, this is one of the reasons PBG cavities fabricated from silicon or other high-index dielectrics can obtain ultrasmall mode volumes. A simple comparison of the mode volume possible in a silicon toroid shows that a mode volume on the order of only about 10 times larger than PBG cavities is possible, with much higher-quality factors. While this work has focused on silica microcavities, the reflow process is a relatively flexible method, thus suggesting that it may be possible to also create high-index ultrahigh-Q quality factor cavities which come closer to the large coupling strengths of PBG cavities while further improving the critical atom number.

Last, the current experimental ability to obtain large coupling strengths with quality factors exceeding 10^8 is promising for the immediate use of these structures in strong-coupling studies. We are currently pressing forward

on improving the fabrication capabilities and losses of these structures. Coupled with the intrinsic fiber-optic compatibility of these structures and the demonstration of near lossless excitation and extraction of optical energy from these structures using tapered optical fibers [17], toroidal microcavities can provide a highly advantageous experimental system for the investigation of strong-coupling cavity QED.

ACKNOWLEDGMENTS

The work of K.J.V. was supported by DARPA, the Caltech Lee Center, and the National Science Foundation. The work of H.J.K. was supported by the National Science Foundation, by the Caltech MURI Center for Quantum Networks, by the Advanced Research and Development Activity, and by the California Institute of Technology.

[1] H. J. Kimble, Phys. Scr. **T76**, 127 (1998).
[2] *Cavity Quantum Electrodynamics*, edited by P. R. Berman (Academic Press, San Diego, 1994).
[3] H. Mabuchi and A. C. Doherty, Science **298**, 1372 (2002).
[4] C. J. Hood, T. W. Lynn, A. C. Doherty, A. S. Parkins, and H. J. Kimble, Science **287**, 1447 (2000).
[5] P. W. H. Pinkse, T. Fischer, P. Maunz, and G. Rempe, Nature (London) **404**, 365 (2000).
[6] Y. Shimizu, N. Shiokawa, N. Yamamoto, M. Kozuma, T. Kuga, L. Deng, and E. W. Hagley, Phys. Rev. Lett. **89**, 233001 (2002).
[7] J. McKeever, J. R. Buck, A. D. Boozer, A. Kuzmich, H.-C. Naegerl, D. M. Stamper-Kurn, and H. J. Kimble, Phys. Rev. Lett. **90**, 133602 (2003).
[8] P. Maunz, T. Puppe, I. Schuster, N. Syassen, P. W. H. Pinkse, and G. Rempe, Nature (London) **428**, 50 (2004).
[9] J. A. Sauer, K. M. Fortier, M. S. Chang, C. D. Hamley, and M. S. Chapman, Phys. Rev. A **69**, 051804(R) (2004).
[10] J. McKeever, A. Boca, A. D. Boozer, J. R. Buck, and H. J. Kimble, Nature (London) **425**, 268 (2003).
[11] V. B. Braginsky, M. L. Gorodetsky, and V. S. Ilchenko, Phys. Lett. A **137**, 393 (1989).
[12] For a recent review of microcavities, see K. J. Vahala, Nature (London) **424**, 839 (2003) and references therein.
[13] M. L. Gorodetsky, A. A. Savchenkov, and V. S. Ilchenko, Opt. Lett. **21**, 453 (1996).
[14] D. W. Vernooy, V. S. Ilchenko, H. Mabuchi, E. W. Streed, and H. J. Kimble, Opt. Lett. **23**, 247 (1998).
[15] V. Lefevre-Seguin and S. Haroche, Mater. Sci. Eng., B **48**, 53 (1997).
[16] D. W. Vernooy, A. Furusawa, N. P. Georgiades, V. S. Ilchenko, and H. J. Kimble, Phys. Rev. A **57**, R2293 (1998).
[17] S. M. Spillane, T. J. Kippenberg, O. J. Painter, and K. J. Vahala, Phys. Rev. Lett. **91**, 043902 (2003).
[18] J. I. Cirac, P. Zoller, H. J. Kimble, and H. Mabuchi, Phys. Rev. Lett. **78**, 3221 (1997).
[19] D. K. Armani, T. J. Kippenberg, S. M. Spillane, and K. J. Vahala, Nature (London) **421**, 925 (2003).
[20] C. J. Hood, H. J. Kimble, and J. Ye, Phys. Rev. A **64**, 033804 (2001).
[21] J. Vuckovic, M. Loncar, H. Mabuchi, and A. Scherer, Phys. Rev. E **65**, 016608 (2001).
[22] B. Lev, K. Srinivasan, P. Barclay, O. Painter, and H. Mabuchi, Nanotechnology **15**, S556 (2004).
[23] J. R. Buck and H. J. Kimble, Phys. Rev. A **67**, 033806 (2003).
[24] T. J. Kippenberg, S. M. Spillane, and K. J. Vahala, Appl. Phys. Lett. **85**, 6113 (2004).
[25] H. Mabuchi and H. J. Kimble, Opt. Lett. **19**, 749 (1994).
[26] D. W. Vernooy and H. J. Kimble, Phys. Rev. A **55**, 1239 (1997).
[27] J. A. Stratton, *Electromagnetic Theory* (McGraw Hill, New York, 1997).
[28] A. W. Snyder and J. D. Love, *Optical Waveguide Theory* (Chapman and Hall, London, 1983).
[29] L. A. Weinstein, *Open Resonators and Open Waveguides* (Golem, Boulder, CO, 1969).
[30] M. L. Gorodetsky, A. A. Savchenkov, and V. S. Ilchenko, Opt. Lett. **21**, 453 (1996).
[31] M. L. Gorodetsky, A. D. Pryamikov, and V. S. Ilchenko, J. Opt. Soc. Am. B **17**, 1051 (2000).
[32] S. M. Spillane, T. J. Kippenberg, and K. J. Vahala, Nature (London) **415**, 621 (2002).
[33] Y. Akahane, T. Asano, B.-S. Song, and S. Noda, Nature (London) **425**, 944 (2003).
[34] W. Hansel, P. Hommelhoff, T. W. Hansch, and J. Reichel, Nature (London) **413**, 498 (2001).
[35] A coupling efficiency of 97% between a fiber-taper and a photonic crystal waveguide has been demonstrated [P. E. Barclay, K. Srinivasan, M. Borselli, and O. J. Painter, Opt. Lett. **29**, 697 (2004)]. For a photonic crystal defect cavity the currently demonstrated efficiency is 44% (P. E. Barclay, K. Srinivasan, and O. J. Painter, http://arxiv.org/abs/physics/0405064).